Structural transformation of Ga_2O_3-based catalysts during photoinduced reforming of methanol

Materials Research Bulletin, Volume 95, November 2017, Pages 71-78

Ádám Vass, Zoltán Pászti, Szabolcs Bálint, Péter Németh, András Tompos, Emília Tálas

http://dx.doi.org/10.1016/j.materresbull.2017.06.034

SSN: 00255408, CODEN: MRBUA, Source Type: Journal Original language: English

DOI: 10.1016/j.materresbull.2017.06.034

Document Type: Article

Publisher: Elsevier Ltd

Corresponding author: Emília Tálas

Highlights

- β-Ga_2O_3 is active in the methanol photocatalytic reforming under UV–vis irradiation.
- PtO_x co-catalyst is formed on the surface of Ga_2O_3 by calcination of $Pt(NH_3)_4(NO_3)_2$.
- Introduction of PtO_x co-catalyst results in enhanced hydrogen production.
- In-situ metallic Pt formation during the photoinduced reaction is proved by XPS.
- PtO_x/Ga_2O_3 transforms to Pt^0/GaOOH during the photoinduced reaction.

Graphical abstract:

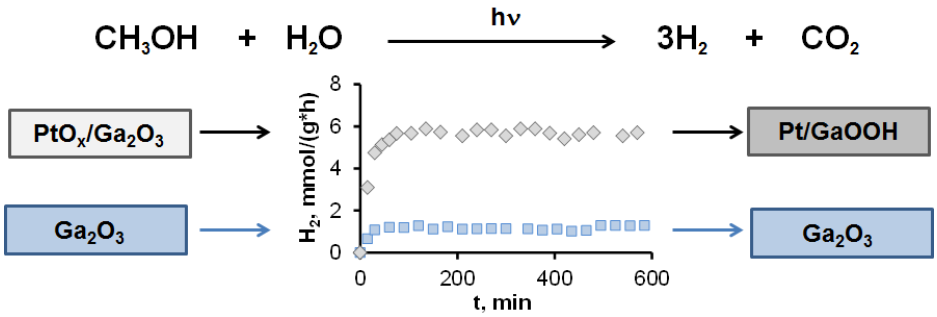

Structural transformation of Ga_2O_3-based catalysts during photoinduced reforming of methanol

Ádám Vass[1], Zoltán Pászti[1], Szabolcs Bálint[1, 2], Péter Németh[1], András Tompos[1], Emília Tálas[1,*]

[1]Institute of Materials and Environmental Chemistry, Research Centre for Natural Sciences, Hungarian Academy of Sciences, H-1117 Budapest, Magyar tudósok körútja 2, Hungary
[2]Semilab Semiconductor Physics Laboratory, H-1117 Budapest, Prielle Kornélia utca 2, Hungary

Abstract

In this work PtO_x/β-Ga_2O_3 is prepared and characterized in order to test its properties in the photoinduced methanol reforming reaction using UV-visible irradiation. XRD, TEM and XPS techniques are used to characterize the fresh and recovered Pt-containing and Pt -free samples. Our results prove that in the presence of Pt the Ga_2O_3 is converted into GaOOH as a result of the irradiation and/or *in situ* photoinduced H_2 formation. In parallel, Pt is gradually reduced and the unusually low value of the $4f_{7/2}$ binding energy of the metallic Pt component evidences electron transfer from GaOOH towards Pt in accordance with its role as cocatalyst.

Keywords: A.gallium oxides; C.X-ray diffraction; C.photoelectron spectroscopy; D.catalytic properties; D.surface properties

[*]Corresponding author, Tel.: +36 1 382 6916, email: talas.emilia@ttk.mta.hu, address: H-1519 Budapest, P.O.Box 286, Hungary (Emília Tálas)

1. Introduction

Due to its favorable electronical and optical properties, Ga_2O_3 is regarded as a promising material for several applications in electronic [1,2] or optoelectronic devices [3], photodetectors [4,5] and sensors [2,6-9]. The large band gap energy (4.8 eV) of Ga_2O_3 [2] contributes to its superior photocatalytic performance [10,11]. The Ga_2O_3-based photocatalysts show exceptional activity in photocatalytic oxidation reactions [11]. Nowadays oxidative degradation of volatile organic compounds (VOCs) into harmless compounds such as carbon dioxide and water has special importance. Pure Ga_2O_3 is highly photoactive for the complete oxidation of gaseous benzene, toluene and ethylbenzene at room temperature without the problem of catalyst deactivation, *i.e.*, the destruction of stable reaction intermediates on Ga_2O_3 maintains of a clean surface on the photocatalyst [10,11]. Ga_2O_3-based materials are suitable to degrade pollutants in aqueous phase, as well (*e.g.* photocatalytic reduction of perfluorooctanoic acid [12,13], photocatalytic oxidation of cyanide [14]). In the activity test of the Ga_2O_3-based photocatalysts, chemicals such as Rhodamine B [15], methylene blue [16], salicylic acid [17] are commonly used as model compounds.

Besides degradation reactions, Ga_2O_3-based photocatalysts are active in non-oxidative coupling reaction of methane [18], in photocatalytic reduction of CO_2 with methane [19] or with water [20], in photocatalytic steam reforming of methane [21] and in photocatalytic water splitting [22-25]. The targeted product of the latter processes is H_2, a promising alternative energy carrier [26]. Methanol photocatalytic reforming reaction [27] (1) is also a possible approach for H_2 production.

$$CH_3OH + H_2O \xrightleftharpoons{\text{Photocatalyst, h}\nu} 3\,H_2 + CO_2 \qquad (1)$$

It is known that metal oxide or metal nanoparticles loaded onto the surface of the semiconductor improve the efficiency of photocatalysts as they promote the charge separation and suppress the recombination of the photogenerated electron-hole pair [28,29]. Another important role of the cocatalyst is to provide reaction sites for elementary reaction steps subsequent to light absorption [21,29]. The latest is particularly important in the photocatalytic hydrogen production, because the cocatalyst has to provide active sites for H^+ reduction and the combination of surface hydrogen atoms into molecular H_2. These steps are less supported by the semiconductor, for example the activity of TiO_2 in reaction (1) can be increased at least an order of magnitude if a proper cocatalyst is involved [30-32].

Reviewing the different cocatalysts applied for Ga_2O_3-based photocatalysts, Ag has been described as effective one in the photocatalytic reduction of CO_2 with water resulting in a mixture of CO and H_2 [20]. NiO [22] and $Rh_{2-y}Cr_yO_3$ [22,23] worked well in water splitting . Photocatalytic steam reforming of methane resulting in H_2 and CO_2 was successfully carried out over Ga_2O_3 in the presence of Pt or Rh cocatalyst [21,33]. Shimura and coworkers studied in detail the role of cocatalysts obtained from different metals by different methods (*i.e.* photodeposition, impregnation followed by calcination, impregnation followed by calcination and successive hydrogen reduction) in the photocatalytic steam reforming reaction [21]. The following order of activity was found: Pt>Rh>Au>Pd>Ni [21]. It was also observed that the different metals gave their maximum activity at different cocatalyst formation method. Upon using Pt cocatalysts the highest activity was obtained if it was prepared by impregnation followed by calcination in air [21]. In our previous work on using Ga-Zn oxynitrides for methanol photocatalytic reforming, we also found that Pt cocatalyst formation by calcination was more favorable than that by high temperature H_2 treatment [34]. However, the presence of Pt cocatalyst in any form resulted in a transformation of the oxynitride phase into oxyhydroxide during the photoinduced reaction [34].

The naturally arising question is to assess the stability of gallium oxide against oxyhydroxide transformation. The present work is aimed to study the performance of PtO_x/β-Ga_2O_3 catalyst system in the photoinduced reforming reaction of methanol (1) and to get knowledge about the reaction induced structural changes of the solid.

2. Materials and methods

2.1 Materials

Aldrich β-Ga_2O_3 (BET specific surface area 8.9 m^2/g) and $Pt(NH_3)_4(NO_3)_2$, Reanal methanol and double distilled water (18 MΩ) were used for the synthesis. As a co-catalyst, 1 w% Pt was loaded onto the β-Ga_2O_3 by incipient wetness impregnation method from the aqueous solution of $Pt(NH_3)_4(NO_3)_2$. After overnight drying at 90°C, the sample was heated up to 300 °C in air using 2 °C/min heating rate and calcined for 1h at 300°C in an oven.

2.2 Hydrogen evolution reaction

The photoinduced reforming reaction was carried out similarly to our previous study [34]. An UV-Consultig Peschl UV-Reactor System 1 equipped with gas inputs and outputs was used as a photoreactor. The measurement of H_2 evolution was carried out in a dynamic system. Nitrogen gas with 20 ml/min flow rate was continuously bubbled through the reactor and a sample from the gas outlet was introduced into the gas chromatograph (GC) by a sampling valve in every fifteen minutes. A GC (Agilent 7820A) equipped with SUPELCO Carboxen 1010 column and TCD detector was used to follow the H_2 production. The internal standard of the GC analysis was argon gas added to the vapor-gas mixture before the GC sampling valve. The H_2 production expressed as H_2 production rate (mmol/(g_{cat}*h)) was corrected by data of direct photolysis in the absence of the Ga-oxide based materials. Initial concentration of methanol was 6 vol% in double distilled water. The reaction was carried out at 30-35°C. The amount of catalyst and the reaction volume were 100 mg and 370 ml, respectively. A mercury medium pressure lamp TQ 150 operating in UV-visible region was used as light source. We monitored the reactions at least for 10 h. After the photoreaction, the samples were recovered from the aqueous methanol solution by centrifuging, washing with 3x50 ml absolute ethanol followed by drying under N_2 flow.

2.3 Characterization of the Ga-oxide based materials

X-ray powder diffraction (XRD) patterns were obtained in a Philips model PW 3710 based PW 1050 Bragg-Brentano parafocusing goniometer using CuK_α radiation (λ= 0.15418 nm), graphite monochromator and proportional counter. During phase analysis we used reference cards from the ICDD PDF-2 (1998) data base. Crystallite sizes were calculated from reflection line broadening using the Scherrer-equation.

Transmission electron microscopy (TEM) studies of the samples were carried out in a FEI Morgagni 268D type transmission electron microscope (accelerating voltage: 100 kV, W-filament). The samples were prepared by grinding and dispersing of the resulted powder in ethanol using an ultrasonic bath.

X-ray photoelectron spectroscopy (XPS) measurements were carried out using an EA125 electron spectrometer manufactured by OMICRON Nanotechnology GmbH (Germany). In order to overcome difficulties due to overlap of the C 1s line with Ga Auger transitions, the photoelectrons were excited by both MgKα (1253.6 eV) and AlKα (1486.6 eV) radiation. Spectra were recorded in the Constant Analyzer Energy mode of the energy analyzer with 30 eV pass energy resulting in a spectral resolution around 1 eV. Samples in the form of fine powder were suspended in isopropanol. Drops of this suspension were placed on standard OMICRON sample plates; after evaporation of the solvent coatings

with sufficient adhesion and electric conductivity were obtained. Binding energies were referenced to the hydrocarbon component of the C 1s peak arising from adventitious contamination at 285.0 eV. Since compositional analysis suggested a strongly oxidized/hydroxylated state for the surface, a secondary reference was the Ga $2p_{3/2}$ peak, which was expected around 1118.8 eV in Ga_2O_3 [35]. Data were processed using the CasaXPS software package [36] by fitting the spectra with Gaussian-Lorentzian product peaks after removing a Shirley or linear background. Nominal surface compositions were calculated using the XPS MultiQuant software package [37,38] with the assumption of homogeneous depth distribution for all components. Chemical states were identified by XPS databases [39,40].

3. Results and discussion

3.1 Effect of cocatalyst on the hydrogen production

Figure 1 shows the results of the photoinduced reforming reaction of methanol over Ga_2O_3 with and without PtO_x cocatalyst. The H_2 formation rate-reaction time dependencies have two main parts, the initial period and a plateau in both cases. The plateau of the H_2 evolution rate represents continuous formation of H_2. The gradual increase of the measured hydrogen production rate in the initial period can be explained by at least two reasons: (i) the methanol solution should be first saturated by hydrogen and reach equilibrium for the liquid phase/nitrogen flow before the measurement became relevant to real gas evolution; (ii) the *in situ* formation of catalytically active sites requires some time. The presence of the cocatalyst results in about fivefold increase in the hydrogen production rate in the steady state (plateau region).

In a separate experiment we also checked the persistency of the good H_2 production activity of the Pt-containing sample. After 10 h reaction time the irradiation and the stirring was finished, then the reaction was restarted again the next day. In this case the same level of H_2 production rate could be reached as before with a somewhat sharper initial period which presumable belonged to the equilibration mentioned above.

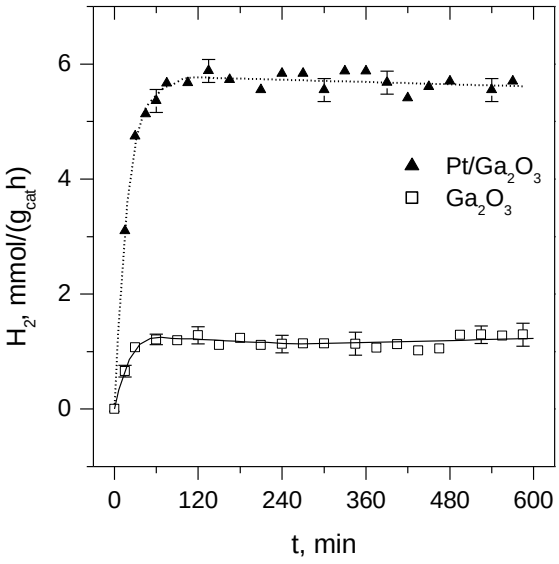

Figure 1. Hydrogen production. □: Ga_2O_3 ▲: PtO_x/Ga_2O_3

3.2 Characterization of the Ga-oxide based materials

In order to obtain a more realistic picture about the structure and the surface of the real working catalyst, results of characterization of the fresh and recovered samples were compared.

3.2.1 Results of XRD measurements

Average particle size of the samples calculated on the basis of XRD is 40-60 nm. The typical XRD patterns of the fresh and recovered Ga_2O_3-based Pt-free and Pt-containing samples are presented in Figure 2. In the absence of the cocatalyst the β-Ga_2O_3 phase does not change during the photoreaction (line b in Figure 2). Similarly, the Pt load does not influence the structure of β-Ga_2O_3 (line c in Figure 2). This finding is consistent with the expectation because β-Ga_2O_3 is considered as the most stable crystalline modification of Ga (III) oxide [2]. However, the structure of the Pt-containing recovered sample shows a drastic difference (*cf.* lines a,b, c and line d in Figure 2); instead of β-Ga_2O_3, the XRD pattern reveals the characteristic peaks of α-GaOOH (# 70-0538) [41-43]. Although α-GaOOH is often used as precursor/intermediate in the preparation of α- and β-Ga_2O_3 [43-46], the reverse reaction, the formation of GaOOH from Ga_2O_3, has not been reported. Instead, the formation of GaOOH is observed in water-rich medium at relative low temperature (<300^{o}C) [42,43,47]. Its finding in our experiments suggests that the presence of Pt can induce the phase transition of β-Ga_2O_3 into GaOOH in the aqueous medium under the long time (600 min) irradiation. The appearance of GaOOH is consistent with our previous finding, *i.e.*, Ga-Zn-oxyhydroxide forms as a result of the photoinduced reforming of methanol over Pt loaded Ga-Zn-oxynitride [34].

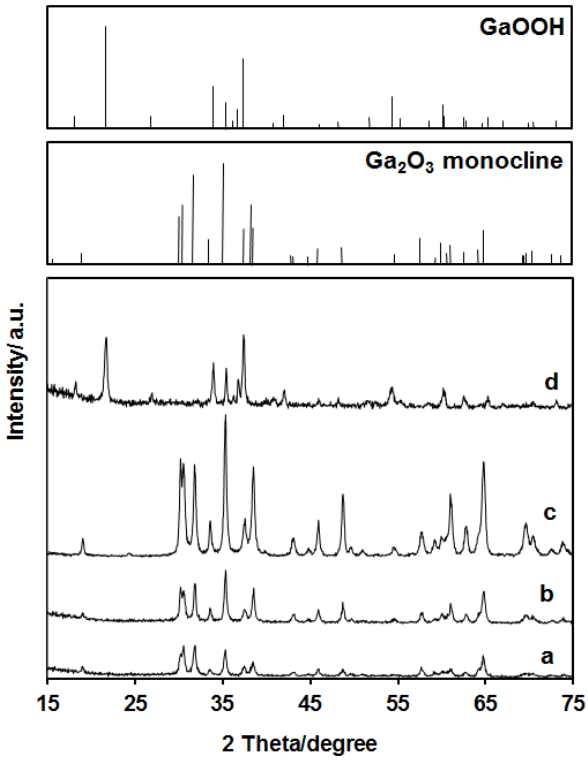

Figure 2. XRD patterns of the β-Ga_2O_3-based samples. a= fresh β-Ga_2O_3; b= Pt-free recovered β-Ga_2O_3; c= fresh PtO_x/β-Ga_2O_3; d= Pt-containing recovered sample (enlarged by factor 3). The elevated background at lower 2theta values for pattern d indicates certain amount of amorphous phase. XRD lines of a, b and c are consistent with monoclinic β- Ga_2O_3 (# 87-1901) and those of d show GaOOH diffractions (# 70-0538).

3.2.2 Results of TEM measurements

The TEM images of the Ga_2O_3-based Pt-free and Pt-containing fresh and recovered samples can be seen in Figure 3.

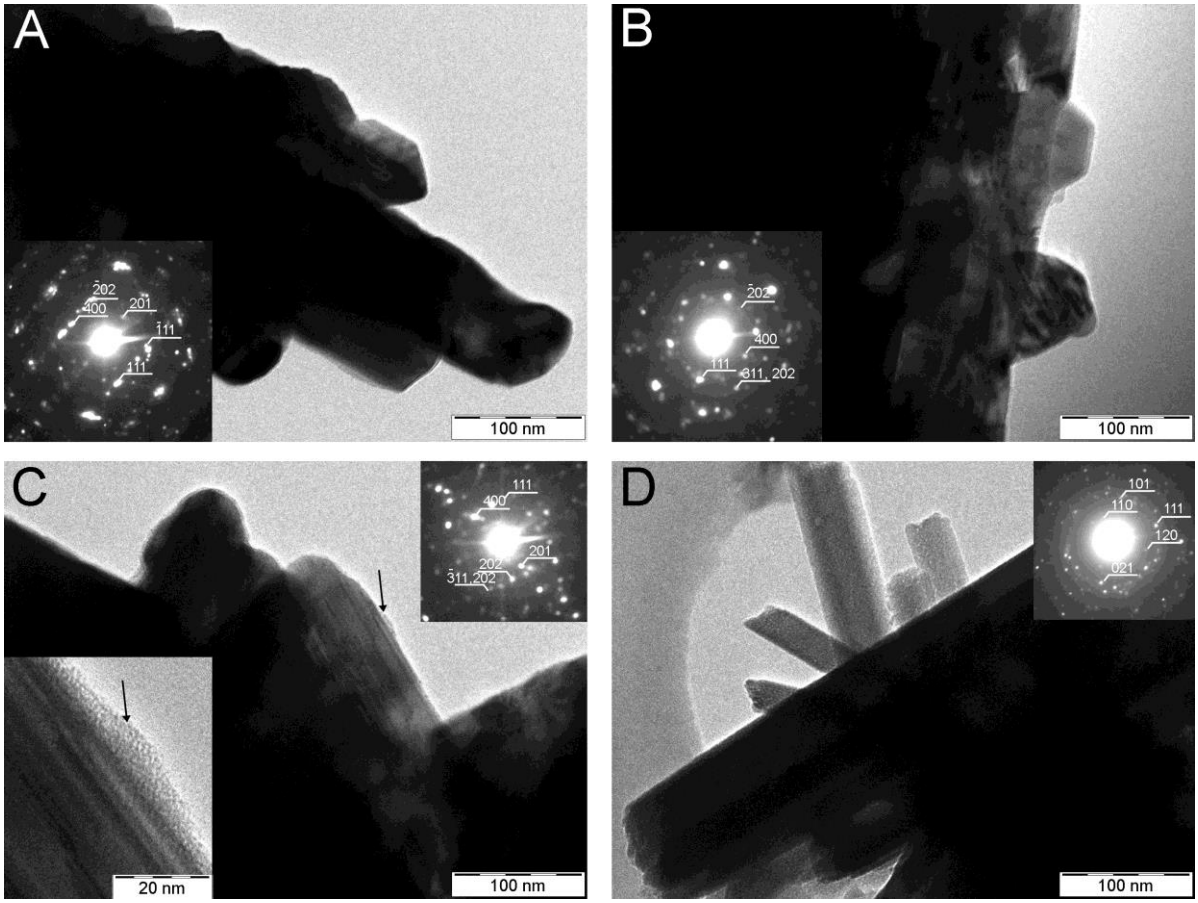

Figure 3. TEM images of the Ga_2O_3-based samples. A: fresh β-Ga_2O_3; B: Pt-free recovered β-Ga_2O_3; C: fresh PtO_x/β-Ga_2O_3; D: Pt-containing recovered sample. Consistently with XRD result, electron diffraction patterns (inserts) show β- Ga_2O_3 (# 87-1901) for A, B, C and GaOOH diffractions (# 70-0538) for D.

The TEM results are in accordance with those of XRD measurements. Fresh β-Ga_2O_3 (Figure 3A), Pt-free recovered β-Ga_2O_3 (Figure 3B) and fresh PtO_x/β-Ga_2O_3 (Figure 3C) samples are very similar to each other; they consist of very large (micrometer-size) rod-like aggregates, which are built up by 50-100 nm crystallites. Formation of the cocatalyst itself does not influence the morphology of the semiconductor; however, the enlarged image of the fresh PtO_x/β-Ga_2O_3 shows the formation of a certain surface layer (black arrow in Figure 3C). We attribute this surface change to Pt introduction. In contrast to Figure 3A, 3B and 3C, Figure 3D shows 20-40 nm wide and 100-500 nm long needle-shape crystals, which, according to their electron diffraction pattern, consist of GaOOH. No sign of the presence of β-Ga_2O_3 is seen in the TEM images or diffraction patterns. We interpret the significant morphological change and the formation of GaOOH to the photoinduced reaction of the Pt-containing sample.

3.2.3 Results of XPS measurements

Table 1 summarizes the most significant XPS data obtained on the studied samples.

Table 1. Characteristic binding energies (in eV) of the Pt 4f, Ga 3d and O 1s levels and Ga/O ratios (in at%/at%) measured by XPS on the samples studied in this work.

Binding energy, eV	Fresh $\beta-Ga_2O_3$	Recovered $\beta-Ga_2O_3$	Impregnated $Pt/\beta-Ga_2O_3$*	Fresh $PtO_x/\beta-Ga_2O_3$; (calcined)	Pt-containing recovered sample
Pt 4f	--	--	72.3	71.2 72.6 73.7	70.8 72.4
Ga 3d	20.5	20.2	20.3	20.4	20.2
O 1s	531.4 533.1	531.3 532.9	531.4 533.1	531.4 533.0	531.2 532.6
Ga/O ratio	0.75	0.65	0.71	0.70	0.53

*1% Pt on the β-Ga_2O_3 by incipient wetness impregnation method from the aqueous solution of $Pt(NH_3)_4(NO_3)_2$ after the overnight drying at 90^oC and before the calcination step.

The Ga 3d peak of the fresh $\beta-Ga_2O_3$ sample can be fitted by a single, relatively narrow component suggesting a single chemical state. The 20.5 eV binding energy corresponds to the fully oxidized Ga [35,39,40]. The Ga/O ratio is somewhat higher than the nominal value for this compound (0.66).

In all studied samples the O 1s peak is decomposed into two contributions. The more intense one appears around 531.2-531.4 eV, which is at the upper end of the range reported for Ga_2O_3 (530.7-531.3 eV [39,40]). The weaker peak around 533 eV can be assigned to surface oxygen containing species like OH groups [48]. In the Ga_2O_3 sample recovered after the photoreaction a small but important shift of the Ga 3d peak is observed towards lower binding energies, while the width of the peak increases only slightly. At the same time, the Ga Auger parameter calculated as the sum of the binding energy of the Ga 3d band and the kinetic energy of the Ga $L_3M_{45}M_{45}$ remains around 1082.6-1082.7 eV, which is generally reported for Ga_2O_3 and indicates that the oxidation state of Ga is still mainly +3. Thus, the surface oxide of the catalyst after the reaction, although still contains Ga^{3+} ions, is different in some sense from the oxide in the Ga_2O_3 system. As the sample was exposed to an aqueous environment, formation of GaOOH on the surface regions is quite plausible. Unfortunately, binding energy data for GaOOH are very scarce in the literature. In Ref. [49] water adsorption on GaAs is investigated. The authors claim that a large dose of water exposure results in a GaOOH-type surface species at Ga 3d binding energy of 20.0 eV. Unfortunately, Ga 3d in Ga_2O_3 is reported also at 20.0 eV in their work. In Ref. [50] water also is studied on GaAs in high pressure XPS experiments. They report a 1.0 eV difference between the Ga $2p_{3/2}$ peak of GaAs and an oxyhydroxide species. Applying the same shift for their Ga 3d data, a binding energy of 20.1 eV is obtained for the oxyhydroxide species. Therefore, the assignment of the Ga 3d peak slightly above 20 eV binding energy to GaOOH seems to be reasonable. The Ga 3d signal arising from $Ga(OH)_3$ occurs around 21.6 eV [35].

The formation of Ga-oxyhydroxide on the surface of the $\beta-Ga_2O_3$ particles during the photochemical experiment is supported by the decreasing Ga/O ratio and the increasing OH-related component in the O 1s spectrum, as depicted in Figure 4, where the O 1s bands of the recovered samples are compared to that of the Ga_2O_3 starting material.

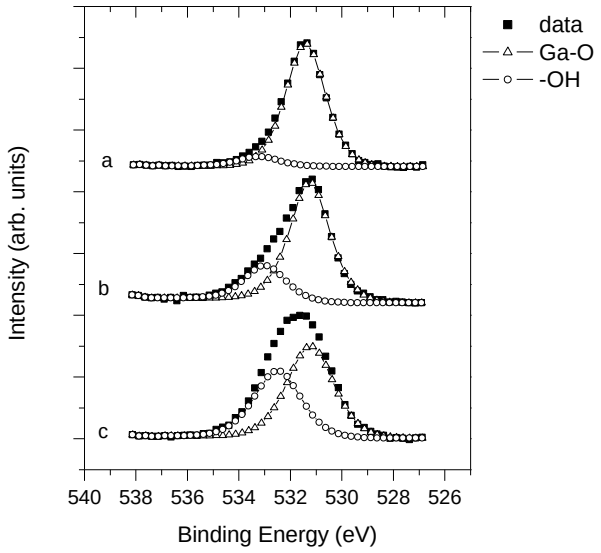

Figure 4. O 1s core level spectra of the different β–Ga_2O_3-based samples. a= fresh β-Ga_2O_3; b= Pt-free recovered β-Ga_2O_3; c= Pt-containing recovered sample.

According to the quantitative evaluation of the XPS data, the Pt content of the Pt-loaded samples is around 1-2 wt%, in good agreement with the intended value. After impregnation the Pt 4f spectrum (see Figure 5) can be conveniently modeled by a broad $4f_{7/2}$-$4f_{5/2}$ doublet, with the $4f_{7/2}$ peak at 72.3 eV. According to the literature, a Pt $4f_{7/2}$ peak between 72-73 eV is due to Pt^{2+} ions (e.g. $Pt(OH)_2$). No signs of metallic Pt (around 71.2 eV binding energy) are found at this stage.

The Ga 3d peak of the impregnated Pt/Ga_2O_3 appears at a somewhat lower binding energy than in the fresh Ga_2O_3 powder. The Ga Auger parameter is consistent with the Ga^{3+} ionic state, while the O 1s spectrum remains essentially identical to that of Ga_2O_3.

Calcination of the sample results in the transformation of the Pt (sample: fresh PtO_x/β-Ga_2O_3 in Table 1). After annealing in air at 300°C, the spectrum is composed of three overlapping doublets, one with its $4f_{7/2}$ peak at 72.6 eV (still due to Pt^{2+} ions), one at 71.2 eV from metallic Pt and a weak contribution at 73.6 eV, arising from Pt^{4+} (like PtO_2) [51,52]. Thus, in spite of the oxidative treatment, calcination results in some reduction of Pt until the metallic state. According to the Ga 3d binding energy and the Ga Auger parameter, the calcined support (sample: fresh PtO_x/Ga_2O_3 in Table 1) essentially consists of Ga_2O_3.

In case of the recovered Pt-containing sample the binding energy shift of the Ga 3d core level is observed again, accompanied by a very significant increase of the oxygen content (decreasing Ga/O ratio) and the appearance of a very intense hydroxyl contribution in the O 1s sample. Since the XRD and the TEM investigations reveal the transformation of the Ga_2O_3 into Ga-oxyhydroxide, it is safe to assign the changes of the Ga binding energy and the O 1s spectrum to the growth of the oxyhydroxide phase.

According to Figure 5, platinum also changes during the photoreaction. The Pt 4f spectrum of the Pt-containing recovered sample can be decomposed into two doublets. The one with the $4f_{7/2}$ peak at 72.4 eV indicates again the presence of Pt^{2+} ions, while the considerably stronger one at 70.8 eV is from metallic Pt.

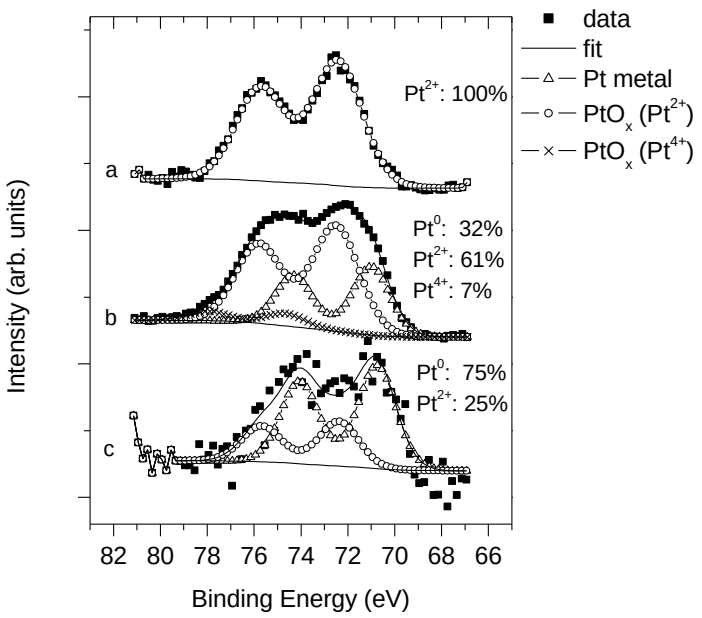

Figure 5: Pt 4f core level spectra for the different Pt-loaded β–Ga_2O_3–based samples. a= Impregnated Pt/Ga_2O_3; b= fresh PtO_x/β-Ga_2O_3 (calcined); c= Pt-containing recovered sample.

The data indicates that in the course of the photoinduced methanol reforming reaction a gradual Pt reduction takes place, thus the cocatalyst develops under the reaction conditions. This observation is in accordance of our previous results obtained on Ga-Zn-oxyhydroxides [34]. Another interesting observation is the unusually low Pt $4f_{7/2}$ binding energy, which probably suggests an electron transfer from the Ga-oxyhydroxide semiconductor towards the metal, in good agreement with the intended effect of the cocatalyst.

3.3 On the photocatalytic nature of the photoinduced methanol reforming reaction

Although it is tempting to identify the observed hydrogen generation under illumination as a result of photocatalytic reforming of methanol, a heterogeneous photochemical process must fulfill several requirements before it can be recognized as a photocatalytic one [53-54]. The most stringent of them is that the product of the photoreaction must leave the active site to restore its original chemical state and make it available for a subsequent reaction, which results in a turnover number (TON) higher than one. If the TON is not larger than unity, the photoinduced reaction cannot be regarded as photocatalytic one [53]. Since calculation of the TON requires the knowledge of the amount of active sites in the sample, which is very difficult to determine under ordinary experimental conditions, a lower limiting value based on the total number of regular surface sites may be used in judging the nature of a photoreaction [53]. The surface lattice ion concentration for monocline Ga_2O_3 is $2.16*10^{19}$ atom/m^2 which is in same order of magnitude that is suggested for calculation by Emeline et al. [53]. Taking into account the BET specific surface area for bare Ga_2O_3, the lower limiting value of TON of 8.0 was obtained which suggest that Ga_2O_3 behaved indeed as a real photocatalyst.

Since the PtO_x/Ga_2O_3 system undergoes a structural transformation, it obviously fails to conform to the definition of being a photocatalyst. On the other hand, as the constant H_2 evolution activity was maintained during the experiment in case of the Pt containing sample, a question arises whether the newly formed solid system can be recognized as photocatalyst or not. The specific surface area of the *in situ* formed PtO_x/GaOOH as well as the reaction time

at which the total transformation of Ga_2O_3 into GaOOH took place is not available so we can only use the total number of Ga atoms introduced with PtO_x/Ga_2O_3 sample as a very rough estimation of a certain kind of lower limiting value of TON, which is 1.2. This value implies the possibility of a photocatalytic process in case of our Pt containing sample, too. Nevertheless, confirmation if the photoinduced reforming of methanol over the transformed PtO_x/GaOOH is indeed a catalytic process requires further work.

3.4 Role of the cocatalyst in the photoinduced methanol reforming reaction

According to the widely accepted opinions the advantages of the cocatalysts in a heterogeneous photoreaction on a semiconductor surface can be attributed to the reduced charge recombination; promoted charge separation and transport driven by junctions/interfaces. Metallic nanoparticles such as Pt^0 direct the photogenerated electrons while metal oxides such us RuO_2 direct the photogenerated holes to the surface of the semiconductor [28, 29]. Another important role of the cocatalyst is to provide reaction sites for elementary reaction steps subsequent to light absorption, such as formation of molecular hydrogen and its desorption from the surface [28,29]. It has been described that different types of photocatalysts containing cocatalyst in form of Pt^0 are more active than the Pt-free ones. Our observations on Pt^0/TiO_2 [55] catalysts obtained by high temperature hydrogen treatment from Pt-precursor salt coincide with the above statement. Our opinion is that Pt^0 is a definitely active cocatalyst. However we could not separate the possible effect of Pt^{n+}. As both the methanol (our reactant) and the *in situ* formed hydrogen (our reaction product) are reductive agents, furthermore the irradiation can also contribute to the gradual reduction of the Pt-containing surface moieties, the *in situ* reduction of the Pt-containing surface species cannot be avoided in this system. The synergistic coexistence of metallic Pt and-PtO_x, which may be the result of the calcination, could also be assumed, leading to a dual cocatalyst system *i.e.* the simultaneous presence of a metal and a metal oxide, which was found to be advantageous [56] however we did not find direct evidence for it in our recent work [55].

The hydroxylation of oxide surfaces is a general phenomenon which influences many systems. Our experiments with the Pt-free β-Ga_2O_3 sample pointed to the occurrence of such a process as XPS gave evidence for appearance of surface hydroxyl groups, while bulk-sensitive methods showed no structural changes. At the same time, it is very difficult to make difference between the "surface oxyhydroxides" and the "hydroxylated surface" in case of the recovered Pt-free sample. However, exclusively in case of the Pt containing sample, both bulk- and surface-sensitive methods demonstrated the transformation of β-Ga_2O_3 into crystalline GaOOH revealing the importance of Pt in this process.

In a purely photocatalytic process the rate of reduction and oxidation processes on the the surface of the photocatalyst are equal. If this balance is broken, a secondary (non-photocatalytic) reaction would occur depending on which half-reaction is more efficient [53]. Comparing the half-reactions over bare Ga_2O_3 and the Pt containing sample the reduction of H^+ with the photogenerated electron would be accelerated by Pt as Pt is known as one of the best catalysts for the reduction of proton. It is conceivable therefore that the presence of Pt contributed to a secondary surface chemical reaction leading to transformation of Ga_2O_3 into the oxyhydroxide.

3.5 The oxyhydroxides as possible photocatalysts

As it was mentioned previously, we have indications that the transformed PtO_x/GaOOH system acts as a photocatalyst, even if an unequivocal proof is not available. Nevertheless, we believe it is worth to discuss the possible role of oxyhydroxides in photocatalysis using several examples from the literature.

Photodeposited amorphous oxyhydroxide layers behave as molecular sieves, which selectively filter the reactant and product molecules on the surface of the semiconductor preventing the oxygen reduction and resulting in successful overall water splitting [57]. The as-prepared InOOH shows photocatalytic activity for benzene degradation [58]. Band gap of InOOH hollow spheres is estimated from the UV-vis diffuse reflectance spectrum to be 3.5 eV, which is almost equal to that of indium oxide-hollow spheres [59]. The suspensions of as-prepared ultrathin β-CoOOH nanosheets can directly photocatalyze hydrogen evolution in a high rate and large quantum efficiencies [60]. However, the photocatalytic activity of bulk oxyhydroxide material is found to be poor [25,60]. It should also be mentioned that in case of the catalyst for water splitting reaction prepared by electrodepositions from Co^{2+} solutions in phosphate electrolytes an *in situ* formed cobalt oxyhydroxide (CoOOH) layer is suggested to be the catalytic active component [61,62].

Based on the previous examples, we think it imaginable that *in situ* formed GaOOH and metallic Pt nanoparticles occurring side-by-side are beneficial for the methanol photocatalytic reforming reaction however this idea need further proofs.

4. Conclusion

In this work the photoinduced reforming of methanol over Ga_2O_3 and PtO_x-loaded Ga_2O_3 was compared. Ga_2O_3 provided notable hydrogen generation in a photocatalytic process. Although the Pt-containing material resulted in considerably higher hydrogen generation rate, XPS data in accordance with the results of XRD and TEM measurements indicated that Ga_2O_3 became converted into GaOOH as a result of the irradiation and/or *in situ* H_2 formation. In parallel, Pt was gradually reduced, while unusually low value of the $4f_{7/2}$ binding energy of the metallic Pt component revealed the electron-rich environmental of the Pt particles, which suggests electron transfer from GaOOH towards Pt in accordance with the role of the cocatalyst. The transformation of the semiconductor during the photoreaction precludes recognition of PtO_x/Ga_2O_3 as a photocatalyst. At the same time, a possible phototcatalytic effect is suggested for the *in situ* formed PtO_x/GaOOH system, although its confirmation needs further studies.

Acknowledgement

This project has been supported by the National Development Agency, grant No. KTIA_AIK_12-1-2012-0014. Financial support by the OTKA-project K77720 (András Tompos) and K100793 (Zoltán Pászti) is greatly acknowledged. Szabolcs Bálint and Péter Németh acknowledge support from János Bolyai Research Fellowship. The authors thank Ms. Ildikó Turi for the technical assistance.

References

[1] M. Hong, W.C. Lee, M.L. Huang, Y.C. Chang, T.D. Lin, Y.J. Lee, J. Kwo, C.H. Hsu, H.Y. Lee, Defining new frontiers in electronic devices with high κ dielectrics and interfacial engineering, Thin Solid Films 515 (2007) 5581–5586.

[2] S.I. Stepanov, V.I. Nikolaev, V.E. Bougrov, A.E. Romanov, Gallium oxide: properties and applications-a review, Rev. Adv. Mater. Sci. 44 (2016) 63-86 and the references cited herein.

[3] Y. Tomm, J.M. Ko, A. Yoshikawa, T. Fukuda, Floating zone growth of β-Ga_2O_3, A new window material for optoelectronic device applications, Sol. Energ. Mat. Sol. Cells 66 (2001) 369-374.

[4] W.E. Mahmoud, Solar blind avalanche photodetector based on the cation exchange growth of β-Ga_2O_3/SnO_2 bilayer heterostructure thin film, Sol. Energ. Mat. Sol. Cells 152 (2016) 65-72.

[5] X. Chen, K. Liu, Z. Zhang, C. Wang, B. Li, H. Zhao, D. Zhao, D. Shen, Self-powered solar-blind photodetector with fast response based on Au/β-Ga_2O_3 nanowires array film Schottky junction. ACS Appl. Mater. Interfaces 8 (2016) 4185–4191.
[6] S. Nakagomi, T. Sai, Y. Kokubun, Hydrogen gas sensor with self-temperature compensation based on β-Ga_2O_3 thin film, Sens. Actuators B 187 (2013) 413– 419.
[7] D. Wang, Y. Lou, R. Wang, P. Wang, X. Zheng, Y. Zhang, N. Jiang, Humidity sensor based on Ga_2O_3 nanorods doped with Na^+ and K^+ from GaN powder, Ceram. Int. 41 (2015) 14790–14797.
[8] O. Lupan, T. Braniste, M. Deng, L. Ghimpu, I. Paulowicz, Y. K. Mishra, L. Kienle, R. Adelung, I. Tiginyanu, Rapid switching and ultra-responsive nanosensors based on individual shell–core Ga_2O_3/GaN:O_x@SnO_2 nanobelt with nanocrystalline shell in mixed phases, Sens. Actuators B 221 (2015) 544-555.
[9] L. Mazeina, Y.N. Picard, S.I. Maximenko, F.K. Perkins, E.R. Glaser, M.E. Twigg, J.A. Freitas Jr., S.M. Prokes, Growth of Sn-doped β-Ga_2O_3 nanowires and Ga_2O_3-SnO_2 heterostructures for gas sensing applications, Cryst. Growth Des. 9 (2009) 4471–4479.
[10] Y.D. Hou, X.C. Wang, L. Wu, Z.X. Ding, X.Z. Fu, Efficient decomposition of benzene over a β-Ga_2O_3 under ambient condition, Environ. Sci. Technol. 40 (2006) 5799-5803.
[11] Y. Hou, L. Wu, X. Wang, Z. Ding, Z. Li, X. Fu, Photocatalytic performance of α-, β-, and γ -Ga_2O_3 for the destruction of volatile aromatic pollutants in air, J. Catal. 250 (2007) 12-18.
[12] B. Zhao, P. Zhang, Photocatalytic decomposition of perfluorooctanoic acid with β-Ga_2O_3 wide bandgap photocatalyst, Catal. Commun. 10 (2009) 1184–1187.
[13] B. Zhao, Mou Lv, L. Zhou, Photocatalytic degradation of perfluorooctanoic acid with β-Ga_2O_3 in anoxic aqueous solution, J. Environ. Sci. 24 (2012) 774–780.
[14] E.S. Baeissa, R.M. Mohamed, Pt/Ga_2O_3–SiO_2 nanoparticles for efficient visible-light photocatalysis, Ceram. Internat.40 (2014) 841–847.
[15] K. Girija, S. Thirumalairajan, D. Mangalaraj, Morphology controllable synthesis of parallely arranged single-crystalline β-Ga_2O_3 nanorods for photocatalytic and antimicrobial activities, Chem. Eng. J. 236 (2014) 181–190.
[16] S.H. Mohamed, M. El-Hagary, S. Althoyaib, Growth of β-Ga_2O_3 nanowires and their photocatalytic and optical properties using Pt as a catalyst, J. Alloys Compd. 537 (2012) 291–296.
[17] Y. Hou, J.Zhang, Z. Ding, L. Wu, Synthesis, characterization and photocatalytic activity of β-Ga_2O_3 nanostructures, Powder Technol. 203 (2010) 440–446.
[18] L. Yuliati, T. Hattori, H. Itoh, H. Yoshida, Photocatalytic nonoxidative coupling of methane on gallium oxide and silica-supported gallium oxide, J. Catal. 257 (2008) 396–402.
[19] L. Yuliati, H. Itoh, H. Yoshida, Photocatalytic conversion of methane and carbon dioxide over gallium oxide, Chem. Phys. Lett. 452 (2008) 178–182.
[20] M. Yamamoto, T. Yoshida, N. Yamamoto, T. Nomoto, S. Yagi, The loading effect of silver nanoparticles prepared by impregnation and solution plasma methods on the photocatalysis of Ga_2O_3, Nucl. Instrum. Methods Phys. Res., Sect. B, 359 (2015) 64–68.
[21] K. Shimura, T. Yoshida, H. Yoshida, Photocatalytic activation of water and methane over modified gallium oxide for hydrogen production, J. Phys. Chem. C 114 (2010) 11466-11474.
[22] Y. Sakata, Y. Matsuda, T. Yanagida, K. Hirata, H. Imamura, K. Teramura, Effect of metal ion addition in a Ni supported Ga_2O_3 photocatalyst on the photocatalytic overall splitting of H_2O, Catal. Lett. 125 (2008) 22-26.
[23] T. Hisatomi, K. Miyazaki, K. Takanabe, K. Maeda, J. Kubota, Y. Sakata, K. Domen, Isotopic and kinetic assessment of photocatalytic water splitting on Zn-added Ga_2O_3 photocatalyst loaded with $Rh_{2-y}Cr_yO_3$ cocatalyst, Chem. Phys. Lett. 486 (2010) 144–146.

[24] Y. Sakata, Y. Matsuda, T. Nakagawa, R. Yasunaga, H. Imamura, K. Teramura, Remarkable improvement of the photocatalytic activity of Ga_2O_3 towards the overall splitting of H_2O, ChemSusChem 4 (2011) 181–184.
[25] Y. Sakata, T. Nakagawa, Y. Nagamatsu, Y. Matsuda, R. Yasunaga, E. Nakao, H. Imamura, Photocatalytic properties of gallium oxides prepared by precipitation methods toward the overall splitting of H_2O, J. Catal. 310 (2014) 45-50.
[26] L. P. Bicelli, Hydrogen: a clean energy source, Int. J. Hydr. Energy 11 (1986) 555–565.
[27] T.A. Kandiel, R. Dillert, L. Robben, D.W. Bahnemann, Photonic efficiency and mechanism of photocatalytic molecular hydrogen production over platinized titanium dioxide from aqueous methanol solutions, Catal. Today 161 (2011) 196–201.
[28] A.L. Linsebigler, G. Lu, T. Yates, Jr, Photocatalysis on TiO_2 surfaces: principles, mechanisms, and selected results, Chem. Rev. 95 (1995) 735–758.
[29] J. Yang, D. Wang, H. Han, C. Li, Roles of co-catalysts in photocatalysis and photoelectrocatalysis, Acc. Chem. Res. 46 (2013) 1900–1909.
[30] L.S. Al-Mazroai, M. Bowker, P. Davies, A. Dickinson, J. Greaves, D. James, L. Millard, The photocatalytic reforming of methanol, Catal. Today 122 (2007) 46–50.
[31] W. Cui, L. Feng, C. Xu, S. Lu, F. Qiu, Hydrogen production by photocatalytic decomposition of methanol gas on Pt/TiO_2 nano-film, Catal. Commun. 5 (2004) 533–536.
[32] W.C. Lin, W.D. Yang, I.L Huang, T.S. Wu, Z.J. Chung, Hydrogen production from methanol/water photocatalytic decomposition using $Pt/TiO_{2-x}N_x$ catalyst, Energy Fuels 23 (2009) 2192–2196.
[33] K. Shimura, K. Maeda, H. Yoshida, Thermal acceleration of electron migration in gallium oxide photocatalysts, J. Phys. Chem. C 115 (2011) 9041–9047.
[34] Á. Vass, Z. Pászti, Sz. Bálint, P. Németh, G. P. Szíjjártó, A. Tompos, E. Tálas, Structural evolution in Pt/Ga-Zn-oxynitride catalysts for photocatalytic reforming of methanol Mater. Res. Bull. 83 (2016) 65–76.
[35] C.C. Surdu-Bob, S.O. Saied, J. Sullivan, Surface compositional changes in GaAs subjected to argon plasma treatment, Appl. Surf. Sci. 183 (2001) 126–136.
[36] N. Fairley, www.casaxps.com, 2006.
[37] M. Mohai, XPS MultiQuant: Multimodel XPS Quantification Software, Surf. Interface Anal. 36 (2004) 828–832.
[38] M. Mohai, XPS MultiQuant: Multi-model X-ray photoelectron spectroscopy quantification program, Version 3.00.16 (2003) http://www.chemres.hu/aki/XMQpages/XMQhome.htm.
[39] C.D. Wagner, A.V. Naumkin, A. Kraut-Vass, J.W. Allison, C.J. Powell, J.R. Rumble Jr., NIST X-ray Photoelectron Spectroscopy Database, Version 3.4, National Institute of Standards and Technology, Gaithersburg, MD 2003; http://srdata.nist.gov/xps/.
[40] J.F. Moulder, W.F. Stickle, P.E. Sobol, K.D. Bomben, Handbook of X-ray Photoelectron Spectroscopy, Perkin-Elmer Corp. Eden Prairie, Minnesota, USA, 1992.
[41] R. Roy, V.G. Hill, E.F. Osborn, Polymorphism of Ga_2O_3 and the System Ga_2O_3-H_2O, J. Am. Chem. Soc, 74 (1952) 719-722.
[42] M.F. Pye, J.J. Birtill, P.G. Dickens, α-Gallium oxide deuteriohydroxide: a powder neutron diffraction investigation, Acta Acta Crystallogr., Sect. B: Struct. Sci 33 (1977) 3224–3226.
[43] M. Muruganandham, R. Amutha, M.S.M.A Wahed, B. Ahmmad, Y. Kuroda, R.P.S. Suri, J.J. Wu, M.E.T. Sillanpaa, Controlled fabrication of α-GaOOH and α-Ga_2O_3 self-assembly and its superior photocatalytic activity, J. Phys. Chem. C 116 (2012) 44–53.
[44] W. Zhao, Y. Yang, R. Hao, F. Liu, Y. Wang, M. Tan, J. Tang, D. Ren, D. Zhao, Synthesis of mesoporous β-Ga_2O_3 nanorods using PEG as template: Preparation, characterization and photocatalytic properties, J. Hazard. Mater. 192 (2011) 1548–1554.

[45] L. Li, W, Wei, M. Behrens, Synthesis and characterization of α-, β-, and γ-Ga_2O_3 prepared from aqueous solutions by controlled precipitation, Solid State Sci. 14 (2012) 971–981.
[46] S. Krehula, M. Ristić, S. Kubuki, Y. Iida, M. Fabián, S. Musić, The formation and microstructural properties of uniform α-GaOOH particles and their calcination products, J. Alloys Compd 620 (2015) 217–227.
[47] H.Y. Playford, A.C. Hannon, E.R. Barney, R.I. Walton, Structures of uncharacterised Polymorphs of Gallium Oxide from Total Neutron Diffraction, Chem. Eur. J. 19 (2013) 2803–2813.
[48] K. Maeda, K. Teramura, T. Takata, M. Hara, N. Saito, K. Toda, Y. Inoue, H. Kobayashi, K. Domen, Overall water splitting on $(Ga_{1-x}Znx)(N_{1-x}O_x)$ solid solution photocatalyst: Relationship between physical properties and photocatalytic activity, J. Phys. Chem. B. 109 (2005) 20504–20510.
[49] J.M. Epp, J.G. Dillard, Effect of ion bombardment on the chemical reactivity of gallium arsenide (100), Chem. Mater. 1 (1989) 325–330
[50] X. Zhang, S. Ptasinska, Dissociative adsorption of water on an H_2O/GaAs(100) interface: in situ near-ambient pressure XPS studies, J. Phys. Chem. C 118 (2014) 4259-4266.
[51] V. Matolín, I. Matolínová, M. Václavu, I. Khalakhan, M. Vorokhta, R. Fiala, I. Piŝ, Z. Sofer, J. Poltierová-Vejprarová, T. Mori, V. Potin, H. Yoshikawa, S. Ueda, K. Kobayashi, Platinum-doped CeO_2 thin film catalysts prepared by magnetron sputtering, Langmuir 26 (2010) 12824–12831.
[52] F. Şen, G. Gökağac, Different sized platinum nanoparticles supported on carbon: An XPS study on these methanol oxidation catalysts, J. Phys. Chem. C 111 (2007) 5715–5720.
[53] A.V. Emeline, V.K. Ryabchuk, N. Serpone, Photoreactions occurring on metal-oxide surfaces are not all photocatalytic. Description of criteria and conditions for processes to be photocatalytic, Catal. Today 122 (2007) 91–100.
[54] S.E. Braslavsky, A.M. Braun, A.E. Cassano, A.V. Emeline, M.I. Litter, L. Palmisano, V.N. Parmon, N. Serpone, Glossary of terms used in photocatalysis and radiation catalysis (IUPAC Recommendations 2011), Pure Appl. Chem. 83 (2011). 931–1014.
[55] E. Tálas, Z. Pászti, L. Korecz, A. Domján, P. Németh, G.P. Szíjjártó, J. Mihály, A. Tompos, PtO_x-SnO_x-TiO_2catalyst system for methanol photocatalytic reforming: Influence of cocatalysts on the hydrogen production, Catal. Today in press http://dx.doi.org/10.1016/j.cattod.2017.02.009
[56] F. Lin Y. Zang, L. Wang, Y. Zhang, D. Wang, M. Yang J. Yang, B. Zhang, Z. Jiang, C. Li, Highly efficient photocatalytic oxidation of sulfur-containing organic compounds and dyes on TiO_2 with dual cocatalysts Pt and RuO_2, Appl. Catal. B: Environmental 127 (2012) 363–370.
[57] T. Takata, C. Pan, M. Nakabayashi, N. Shibata, K. Domen, Fabrication of a core-shell-type photocatalyst via photodeposition of group IV and V transition metal oxyhydroxides: an effective surface modification method for overall water splitting, J. Am. Chem. Soc. 137 (2015) 9627−9634.
[58] Z. Li, Z. Xie, Y. Zhang, L. Wu, X. Wang, X. Fu, Wide band gap p-block metal oxyhydroxide InOOH: a new durable photocatalyst for benzene degradation, J. Phys. Chem. C 111 (2007) 18348-18352
[59] H.L. Zhu, K.H. Yao, H. Zhang, D.R. Yang, InOOH hollow spheres synthesized by a simple hydrothermal reaction, J. Phys. Chem. B 109 (2005) 20676-20679.
[60] S. He, Y. Huang, J. Huang, W. Liu, T. Yao, S. Jiang, F. Tang, J. Liu, F. Hu, Z. Pan, Q. Liu, Ultrathin CoOOH oxides nanosheets realizing efficient photocatalytic hydrogen evolution, J. Phys. Chem. C 119 (2015) 26362−26366.

[61] Y. Surendranath, M.W. Kanan, D.G. Nocera, Mechanistic studies of the oxygen evolution reaction by a cobalt-phosphate catalyst at neutral pH, J. Am. Chem. Soc. 132 (2010) 16501−16509.
[62] Y. Surendranath, D.A. Lutterman, Y. Liu, D.G. Nocera, Nucleation, growth, and repair of a cobalt-based oxygen evolving catalyst, J. Am. Chem. Soc. 134 (2012) 6326−6336.